Sustainability in Environment
ISSN 2470-637X (Print) ISSN 2470-6388 (Online)
Vol. 10, No. 1, 2025
www.scholink.org/ojs/index.php/se

Original Paper

Multi-objective Scheduling of Microgrids Considering the Curtailment Rate of Renewable Energy

Zhiwei Guo[1*]

[1] College of Railway Transportation, Hunan University of Technology, Zhuzhou Hunan, China

[*] Zhiwei Guo, College of Railway Transportation, Hunan University of Technology, Zhuzhou Hunan, China

Fund Project

Postaraduate Scientific Research Innovation Project of Hunan Province (CX20240920).

Received: January 103, 2025 Accepted: February 13, 2025 Online Published: February 27, 2025

doi:10.22158/se.v10n1p99 URL: http://dx.doi.org/10.22158/se.v10n1p99

Abstract

In order to improve the utilization rate of renewable energy and comprehensively enhance the economic efficiency and environmental friendliness of the microgrid, a multi - objective scheduling model for the microgrid is proposed. The objective functions of this model are to minimize the power generation cost, environmental cost, and wind and solar curtailment cost of the microgrid. The dream optimization algorithm with an adaptive strategy is used to solve the model. Through comparative analysis, it is verified that the proposed model has a better objective trade - off effect compared with single-objective and dual - objective models. Compared with the scenario only considering generation cost and environmental cost, the model can reduce the comprehensive operation cost by 2.9% and lower the wind and solar curtailment cost by 63.44%. Meanwhile, the proposed algorithm is compared with DOA, SSA, GWO, and PSO. It is concluded that the proposed algorithm has advantages in solution quality, stability, and objective trade - off both in test functions and in specific cases.

Keywords

microgrid scheduling, multi-objective, dream optimization algorithm, Renewable energy consumption

1. Introduction

With the increasing attention to environmental issues and power dispatching issues, the development of microgrids (MGs), has been greatly valued (Uddin et al., 2023). MG scheduling optimization faces multiple challenges, especially how to effectively integrate economic efficiency and environmental friendliness in the process of scheduling, which becomes a key challenge in the design of optimization

models. Moreover, the high penetration of renewable energy sources such as wind and solar energy brings significant volatility and uncertainty, which affects the stability and reliability of the power system (Ali et al., 2024). Research on MG optimization models mainly focuses on the economic-environmental. Lin (Lin et al., 2023) taking into account the constraints of the flexibility margin index of renewable resources and aiming to minimize the total operating cost, optimized scheduling strategies for different time scales, such as day-ahead scheduling and intra - day scheduling, are formulated, which reduces the operating cost and the wind curtailment rate. Even if studies like this have taken wind and solar curtailment into account, them usually treat the optimization of wind and solar curtailment cost as a constraint condition. This leads to the complementary advantage of weight distribution among objectives and addresses the issue of insufficient optimization dimensions.

The MG scheduling problem is characterized by multiple objectives and multiple dimensions, making it suitable for solution using computer algorithms. grey wolf optimizer (GWO) (Wang et al., 2020), particle swarm optimization (PSO) (Raghavan et al., 2020), sparrow search algorithm (SSA) (Mortazi et al., 2023) have been applied in the MG scheduling problem. However, these traditional algorithms all have drawbacks such as being prone to getting trapped in local optima and having insufficient convergence accuracy.

In response to the above issues, this paper constructs a three-objective scheduling model for MG that includes generation cost, environmental cost, and wind and solar curtailment cost. Moreover, an improved dream optimization algorithm (DOA) named adaptive dream optimization algorithm (ADOA) with an adaptive strategy is proposed to solve the optimization model. By breaking through the limitations of traditional constraint conditions, the model treats the wind and solar curtailment cost as an independent optimization objective, thus establishing a more comprehensive multi-objective scheduling framework. Finally, through simulation verification, the model and algorithm proposed in this paper can significantly reduce the comprehensive comprehensive operation cost of the MG, and improve the MG's economic performance, environmental friendliness, and clean energy consumption rate.

2. MG Model

This paper considers a MG operates in the grid-connected mode and can conduct power interaction with the Grid. The MG contains distributed generation devices (wind turbines (WT), photovoltaics (PV), microturbines (MT), fuel cells (FC)), and an energy storage system (ESS), and its structure is shown in **Figure 1**.

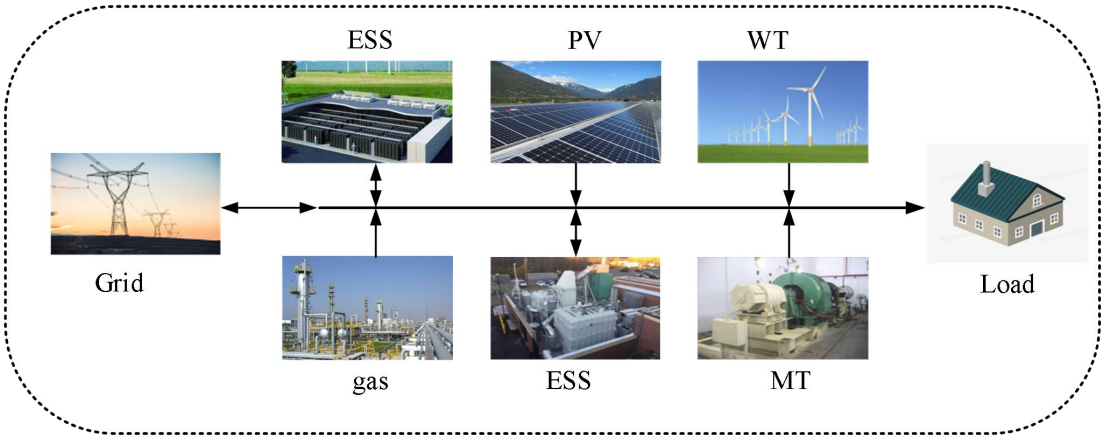

Figure 1. Schematic Diagram of MG Model

2.1 WT Model

$$C_{\mathrm{WT,OM}} = \sum_{t=1}^{T} k_{\mathrm{WT,OM}} P_{\mathrm{WT}}(t) \tag{1}$$

In the above equation, $C_{\mathrm{WT,OM}}$ is the operation and maintenance cost of the WT, $k_{\mathrm{WT,OM}}$ is the unit operation and maintenance cost coefficient of the WT, $P_{\mathrm{WT}}(t)$ is the unit operation and maintenance cost coefficient of the WT, and T is the scheduling cycle.

2.2 PV Model

$$C_{\mathrm{PV,OM}} = \sum_{t=1}^{T} k_{\mathrm{PV,OM}} P_{\mathrm{PV}}(t) \tag{2}$$

In the above equation, $C_{\mathrm{PV,OM}}$ is the operation and maintenance cost of the PV, $k_{\mathrm{PV,OM}}$ is the unit operation and maintenance cost coefficient of the PV, $P_{\mathrm{PV}}(t)$ is the output power of the PV in the tth time period.

2.3 MT Model

The operation and maintenance cost and fuel cost of the MT are as follows.

$$\begin{cases} C_{\mathrm{MT,OM}} = \sum_{t=1}^{T} k_{\mathrm{MT,OM}} P_{\mathrm{MT}}(t) \\ C_{\mathrm{MT,fuel}} = \rho_{gas} \dfrac{1}{LHV} \sum_{t=1}^{T} \dfrac{P_{\mathrm{MT}}(t)}{\eta_{\mathrm{MT}}(t)} \\ \eta_{\mathrm{MT}}(t) = 0.0753 \left(\dfrac{P_{\mathrm{MT}}(t)}{65} \right)^3 - 0.3095 \left(\dfrac{P_{\mathrm{MT}}(t)}{65} \right)^2 + 0.4174 \dfrac{P_{\mathrm{MT}}(t)}{65} + 0.1068 \end{cases} \tag{3}$$

In the above equation, $C_{\mathrm{MT,OM}}$ is the operation and maintenance cost of the MT, $k_{\mathrm{MT,OM}}$ is the operation and maintenance cost of the MT, $C_{\mathrm{MT,fuel}}$ is the fuel cost of the MT； $P_{\mathrm{MT}}(t)$ and $\eta_{\mathrm{MT}}(t)$ are the output power and working efficiency of the MT in the tth time period respectively； ρ_{gas} is the price of natural gas, and LHV is the lower heating value of natural gas.

2.4 FC Model

$$\begin{cases} C_{\mathrm{FC,OM}} = \sum_{t=1}^{T} k_{\mathrm{FC,OM}} P_{\mathrm{FC}}(t) \\ C_{\mathrm{FC,fuel}} = C_{gas} \dfrac{1}{\mathrm{LHV}} \dfrac{\sum_{t=1}^{T} P_{\mathrm{FC}}(t)}{\eta_{\mathrm{FC}}} \end{cases} \tag{4}$$

In the above equation, $C_{\mathrm{FC,OM}}$ is the operation and maintenance cost of the FC, $k_{\mathrm{FC,OM}}$ is the unit operation and maintenance cost coefficient of the FC, $C_{\mathrm{FC,fuel}}$ and $P_{\mathrm{FC}}(t)$ are respectively the fuel cost of the FC and the fuel cost and output power of the FC; η_{FC} is the working efficiency of the FC.

2.5 ESS Model

$$\begin{cases} SOC_{\mathrm{ESS}}(t) = SOC_{\mathrm{ESS}}(t-1) + \left(\eta_{\mathrm{chr}} P_{\mathrm{chr}}(t) I_{\mathrm{chr}}(t) - \dfrac{P_{\mathrm{dis}}(t)}{\eta_{\mathrm{dis}}} I_{\mathrm{dis}}(t) \right) \Delta t \\ I^{i}_{\mathrm{chr}}(t) + I^{i}_{\mathrm{dis}}(t) \le 1 \end{cases} \tag{5}$$

$$C_{\mathrm{ESS,OM}} = k_{\mathrm{ESS,OM}} \sum_{t=1}^{T} \left(P_{\mathrm{chr}}(t) I_{\mathrm{chr}}(t) + P_{\mathrm{dis}}(t) I_{\mathrm{dis}}(t) \right) \tag{6}$$

In the above equation, $SOC_{ESS}(t)$ is the state of charge of the energy storage in the ESS after the end of the tth time period; $P_{chr}(t)$ and $P_{dis}(t)$ are the charging amount and discharging amount of the ESS; η_{chr} and η_{dis} represent the charging efficiency and discharging efficiency of the ESS, $I_{chr}(t)$ and $I_{dis}(t)$ are the charging state flag bit and discharging state flag bit of the ESS. are the charging state flag bit and discharging state flag bit of the ESS, $I_{chr}(t)$=1, $I_{dis}(t)$=0. When the ESS is discharging, $I_{chr}(t)$=0, $I_{dis}(t)$=1. $C_{\mathrm{ESS,OM}}$ is the operation and maintenance cost of the ESS; $k_{\mathrm{ESS,OM}}$ is the unit operation and maintenance cost coefficient of the ESS.

2.6 Demand Response Model

With time-of-use (TOU) electricity pricing, the relationship between the load and the electricity price can be expressed as:

$$L(t) = L_0(t) + L_0(t) E(t,t) \left(\frac{\rho_{\mathrm{buy}}(t) - \rho_{\mathrm{buy0}}(t)}{\rho_{\mathrm{buy0}}(t)} \right) + L_0(t) \sum_{i \ne j}^{24} E(t,h) \left(\frac{\rho_{\mathrm{buy}}(h) - \rho_{\mathrm{buy0}}(h)}{\rho_{\mathrm{buy0}}(h)} \right) \tag{7}$$

In the above equation, $L(t)$ and $L_0(t)$ are the load and the initial load, ρ_{buy0} and ρ_{buy} re the electricity prices before and after the implementation of the TOU electricity pricing, **E** is the price elasticity matrix.

3. Objective Function and Constraints

In order to uniformly coordinate the economic efficiency, environmental friendliness and improve the consumption of wind and solar energy of the system operation, the optimization objective is considered to be minimizing the comprehensive operation cost of the MG. The comprehensive operation cost of the MG includes economic cost, environmental cost, and curtailment cost of wind and photovoltaic power.

3.1 Objective Function

3.1.1 Generation Cost

The generation cost consists of operation and maintenance cost, fuel cost, and power interaction cost.

$$F_1 = \sum_{n=1}^{N} C_{n,\mathrm{OM}} + C_{\mathrm{MT,fuel}} + C_{\mathrm{FC,fuel}} + \rho_{\mathrm{buy}} P_{\mathrm{grid,buy}} - \rho_{\mathrm{sell}} P_{\mathrm{grid,se\ ll}} \tag{8}$$

In the above equation, F_1 is the generation cost, $C_{n,\mathrm{OM}}$ is the operation and maintenance cost of the nth device; N is the total number of devices;; $P_{\mathrm{grid,buy}}$ and $P_{\mathrm{grid,sell}}$ are the interaction powers between the and the Grid. ρ_{buy} and $\rho_{\mathrm{sell}}$are the electricity purchase price and the electricity selling price.

3.1.2 Environmental Cost

The environmental cost refers to the treatment cost of polluting gases generated when the MT, FC and the Grid supply power.

$$F_2 = \sum_{m=1}^{M} \left\{ k_{m,\mathrm{emi}} \lambda_{m,\mathrm{MT}} P_{\mathrm{MT}} + k_{m,\mathrm{emi}} \lambda_{m,\mathrm{FC}} P_{\mathrm{FC}} + k_{m,\ \mathrm{emi}} \lambda_{m,\mathrm{gri\ d}} P_{\mathrm{grid,buy}} \right\} \tag{9}$$

In the above equation, F_2 is the environmental cost, $k_{m,\mathrm{emi}}$ is the pollution emission penalty coefficient of the mth kind of polluting gas, $\lambda_{m,\mathrm{MT}}$, $\lambda_{m,\mathrm{FC}}$ and $\lambda_{m,\mathrm{grid}}$ are the pollution gas emission coefficients when the MT, FC and the Grid generate power.

3.1.3 curtailment Cost

The curtailment cost of wind and photovoltaic power is the cost of the power output of WT and PV that has not been absorbed.

$$F_3 = c_p (P_{\mathrm{PV\_p}} + P_{\mathrm{WT\_p}} - P_{\mathrm{PV}} - P_{\mathrm{WT}}) \tag{10}$$

In the above equation, F_3 is the curtailment cost, c_p is the treatment cost per unit power for curtailed wind and photovoltaic power, $P_{\mathrm{PV\_p}}$, $P_{\mathrm{WT\_p}}$, P_{PV} and P_{WT} are the predicted output powers of the PV and WT and their actual output powers respectively.

3.1.4 Objective Function

The objective function of the multi-objective optimal dispatch problem of the MG is defined as,

$$\min F = w_1 F_1 + w_2 F_2 + w_3 F_3 \tag{11}$$

$$w_1 + w_2 + w_3 = 1 \tag{12}$$

In the above equation, F is the comprehensive operation cost. w_1, w_2, and w_3 are the weights of the generation cost, environmental cost and curtailment cost when calculating the comprehensive operation cost. In this model, it is taken that w_1=w_2=w_3.

3.2 Constraints

3.2.1 Power Balance Constraint

$$L(t) = P_{\mathrm{PV}}(t) + P_{\mathrm{WT}}(t) + P_{\mathrm{DE}}(t) + P_{\mathrm{MT}}(t) + P_{\mathrm{FC}}(t) + P_{\mathrm{grid,buy}}(t) - P_{\mathrm{grid,sell}}(t) + \left(\eta_{\mathrm{chr}} P_{\mathrm{chr}}(t) I_{\mathrm{chr}}(t) - \frac{P_{\mathrm{dis}}(t)}{\eta_{\mathrm{dis}}} I_{\mathrm{dis}}(t) \right) \tag{13}$$

3.2.2 Power Constraint

$$P_n^{\min} \le P_n(t) \le P_n^{\max} \tag{14}$$

In the above equation, $P_n(t)$ is the output power of device, $P_n^{\max}$ 和 $P_n^{\min}$ 分 are the upper and lower limits of the output power per unit time of devices。

3.2.3 Energy Storage Constraint

$$\begin{cases} SOC_{\text{ESS}}^{\min} \le SOC_{\text{ESS}}(t) \le SOC_{\text{ESS}}^{\max} \\ P_{\text{chr}}^{\min} < P_{\text{chr}}(t) S_{\text{chr}}(t) \\ P_{\text{chr}}^{\min} \le P_{\text{chr}}(t) I_{\text{chr}}(t) - P_{\text{chr}}(t-1) I_{\text{chr}}(t-1) \le P_{\text{chr}}^{\max} \\ P_{\text{dis}}^{\min} \le P_{\text{dis}}(t) I_{\text{dis}}(t) - P_{\text{dis}}(t-1) I_{\text{dis}}(t-1) \le P_{\text{dis}}^{\max} \end{cases} \tag{15}$$

In the above equation, $SOC_{\text{ESS}}^{\min}$, $SOC_{\text{ESS}}^{\min}$ are the upper and lower limits of the ESS capacity. $P_{\text{chr}}^{\min}$, $P_{\text{chr}}^{\max}$, $P_{\text{dis}}^{\min}$ and $P_{\text{dis}}^{\max}$ are the upper and lower limits of the charging and discharging power of the ESS.

3.2.4 Ramp Rate Constraint

$$\left| P_n(t) - P_n(t-1) \right| \le R_n \tag{16}$$

In the above equation, R_n is the maximum ramp-up/down power of device n.

3.2.5 Interconnection Line Constraint

$$\begin{cases} P_{\text{grid,buy}}^{\min} \le P_{\text{grid,buy}}(t) \le P_{\text{grid,buy}}^{\max} \\ P_{\text{grid,buy}}^{\min} \le P_{\text{grid,buy}}(t) \le P_{\text{grid,buy}}^{\max} \end{cases} \tag{17}$$

In the above equation, $P_{\text{grid,buy}}^{\max}$, $P_{\text{grid,buy}}^{\min}$, $P_{\text{grid,buy}}^{\max}$ and $P_{\text{grid,buy}}^{\min}$ are the upper and lower limits of the power interaction with the Grid per unit time.

4. Solution Algorithm

4.1 DOA

DOA is a new meta-heuristic algorithm inspired by human dreams. This algorithm divides the optimization process into exploration and exploitation stages, and combines the strategies of partial memory retention, forgetting, and supplementation. It can improve the convergence speed during the exploration stage and enhance the ability to escape from local optima during the exploitation stage (Lang et al., 2025).

4.2 ADOA

The DOA makes individuals execute the forgetting and supplementation strategy or the dream sharing strategy according to a certain forgetting dimension in both the exploration and exploitation stages. Among them, the calculation method of the forgetting dimension is:

$$k_q = randi\left(\frac{Dim}{8\times q}, max\left\{2, \frac{Dim}{3\times q}\right\}\right), \quad q = 1,2,3,4,5 \tag{18}$$

$$k_r = randi\left(2, max\left\{2, \frac{Dim}{3}\right\}\right) \tag{19}$$

In the above equation, k_q represents the number of forgetting dimensions of group q in the exploration stage, k_r is the number of forgetting dimensions in the exploitation stage, Dim is the dimension of the problem. $Randi$ (a, b) is a random integer selected within the range of [a, b].

During the operation of the initial algorithm, the selection of the forgetting dimension is completely random, and the update may not be closely related enough to the historical optimal update relationship in the development process. Considering the addition of an adaptive strategy, in the exploration stage, the statistical information of the population fitness is introduced, and the forgetting dimension is dynamically adjusted according to the improvement degree and diversity of each group of the population. When the population is significantly improved, a larger search range is maintained, and when the population is stagnant, the diversity of the population is dynamically increased according to the iterative process; in the exploitation stage, the forgetting dimension that decreases non-linearly with the iterative process is used.

This adaptive strategy based on renewing information can accurately reflect the search state. During the exploration phase, when the update frequency of the optimal value in each group is high, maintain a high forgetting dimension to enable individuals to search in a broader space. Conversely, reduce the forgetting dimension to focus on local search. As the iterative process progresses, the search range is gradually narrowed to balance global and local searches.

The optimized calculation method of the forgetting dimension is as follows:

$$\begin{cases} k_{q\_\max} = max\left\{2, \dfrac{Dim}{3\times q}\right\} \\ k_{q\_\min} = \dfrac{Dim}{8\times q} \end{cases}, q = 1,2,3,4,5 \tag{20}$$

$$k_q = ceil(k_{q\_\max} - (k_{q\_\max} - k_{q\_\min}) \cdot (\frac{i + I_{\max} - I_d}{I_{\max}}) + cont)^2 \tag{21}$$

$$k_r = max\left\{2, ceil(\frac{Dim}{3} \cdot (1 - \frac{i}{I_{\max}})^2)\right\} \tag{22}$$

In the above equation, $k_{q\_\max}$ and $k_{q\_\min}$ is the maximum and minimum values of the forgetting dimensions of group q in the exploration stage； I, I_d and $I_{\max}$ are the current number of iterations, the maximum number of iterations in the exploration stage, and the total maximum number of iterations. $ceil$(a) represents rounding up the value of a, and $cont$ is the success rate of updating the group's optimal solution for each group in the current iteration.

4.3 Analysis of Algorithms

Using standard test functions for comparison can intuitively reflect the capabilities of the algorithms. In this paper, three typical test functions are selected. Among them, $f_1(x)$ is a unimodal function with only

one optimal solution, and $f_2(x)$ and $f_3(x)$ are multimodal functions, which have several local optimal solutions and one theoretical optimal solution. The information of the test functions is shown in **Table 1**.

Table 1. Test Function

Fuction	Range	d	Theoretical minimum
$f_1(\mathbf{x}) = \sum_{i=1}^{d}\left(\sum_{j=1}^{d}(j+10)\left(x_j^i - \frac{1}{j^i}\right)\right)^2$	[-10,10]	1	0
$f_2(\mathbf{x}) = -\frac{1+\cos\left(12\sqrt{x_1^2+x_2^2}\right)}{0.5(x_1^2+x_2^2)+2}$	[-5.12,5.12]	2	-1
$f_3(\mathbf{x}) = -(x_2+47)\sin\left(\sqrt{\left\|x_2+\frac{x_1}{2}+47\right\|}\right) - x_1\sin\left(\sqrt{\left\|x_1-(x_2+47)\right\|}\right)$	[-512,512]	2	-959.6407

The DOA, PSO, SSA, and GWO algorithms are compared with the ADOA algorithm, and a comparative analysis is carried out from the aspects of convergence accuracy, stability, and convergence speed. To achieve a fair comparison, for all algorithms, the population size is set to 100, the number of iterations is set to 400, and all algorithms are subjected to 20 independent experiments to avoid the randomness of the experiments. The average iteration curves of the five algorithms under the same conditions are shown in **Figures 2**, **3**, and **4**. The best, mean, standard deviations, and average running times of the test results are shown in **Table 2**. The parameter settings of PSO are w = 0.5, c1 = 1.5, and c2 = 1.5. For SSA, ST = 0.2, SD = 0.8, and PD = 0.7. For GWO, $\alpha \in [2, 0]$.

Figures 2, **3**, and **4** depict the evolutionary processes of the five algorithms when solving the optimal solutions of different functions. Although the convergence speed of ADOA slows down, the quality of the obtained optimal solution is higher than that of other algorithms, and there is a significant improvement in the comprehensive solving ability compared with DOA.

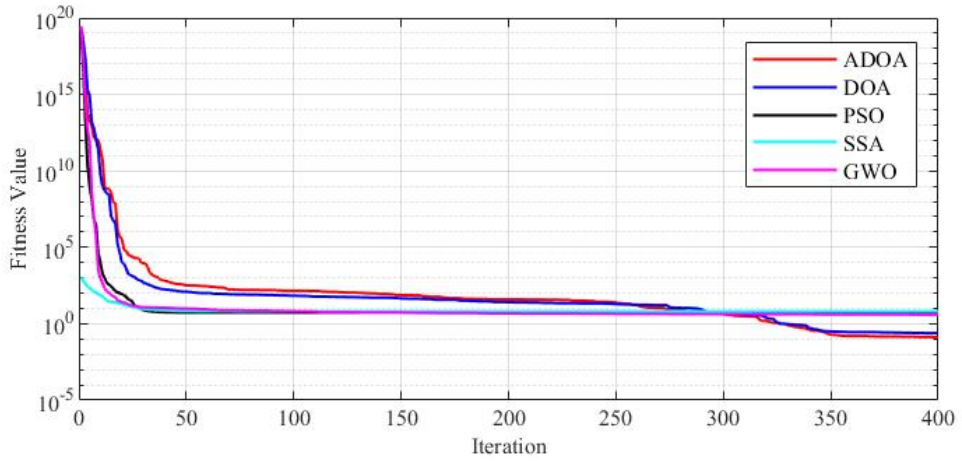

Figure 2. Algorithm Convergence Curve of $f_1(x)$

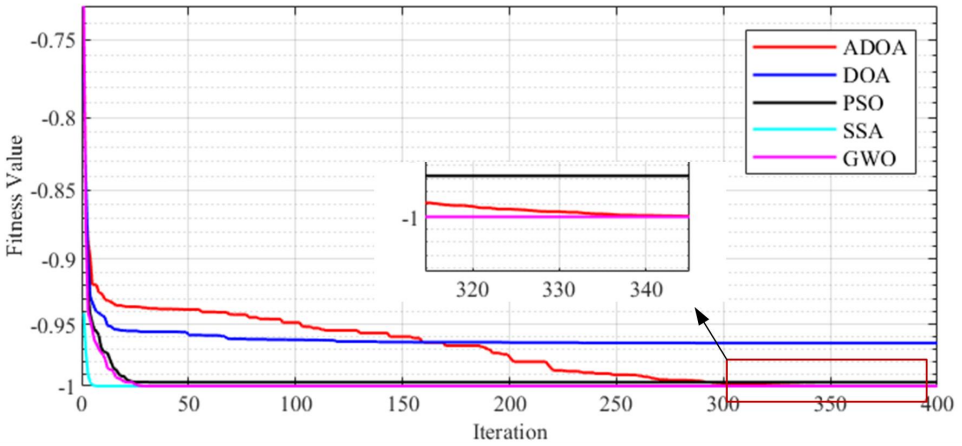

Figure 3. Algorithm Convergence Curve of $f_2(x)$

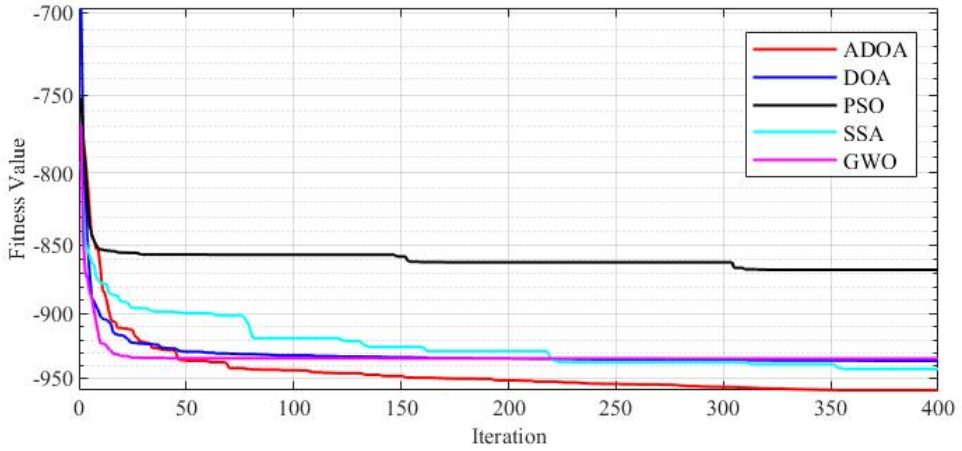

Figure 4. Algorithm Convergence Curve of $f_3(x)$

Table 2. Test Results

Function	Algorithms	Best	Mean	Std	Tmean
$f_1(x)$	ADOA	4.9503E-04	0.1329	0.2148	0.5566
	DOA	5.7372E-04	0.2421	0.5285	0.5588
	PSO	1.8100E-05	5.3608	6.9764	0.5055
	SSA	0.0738	6.4875	6.8274	0.7029
	GWO	0.0811	3.9911	5.9540	0.5222
$f_2(x)$	ADOA	-1	-0.9999	1.1919E-09	0.0217
	DOA	-1	-0.9649	0.0325	0.02178
	PSO	-1	-0.9968	0.0142	0.02126
	SSA	-1	-1	0	0.0826
	GWO	-1	-1	0	0.0253
$f_3(x)$	ADOA	-959.6407	-959.5040	0.6086	0.0227
	DOA	-959.6406	-936.2017	27.0854	0.0224
	PSO	-959.6407	-867.6961	95.9855	0.0237
	SSA	-959.6407	-942.6777	37.6097	0.0828
	GWO	-959.6407	-934.5543	57.4254	0.0269

Table 2 describes the test results of the five algorithms. For $f_1(x)$ and $f_2(x)$, ADOA has advantages in terms of the best, mean, and standard deviation. Although its average running speed is slightly longer than those of PSO and GWO, it has obvious advantages in other indicators and shows the strongest comprehensive superiority. For $f_3(x)$, ADOA still has advantages in the best, mean, and standard deviation, and its average running speed is only second to that of DOA.

Combined with **Figure 4**, although when finding the same optimal solution, the iteration speed of DOA is significantly slower than that of GWO, by comparing the mean, standard deviation, and average running speed, it can be known that the optimization search effect of DOA is more stable and the running speed is faster. From the differences with other algorithms, it can be analyzed that the introduction of the adaptive strategy can improve the local optimization search ability of the DOA algorithm. From the average convergence curve, it can be seen that the adaptive strategy improves the ability to jump out of local optimal solutions, and from the best, mean, and standard deviation, it can be known that adding the adaptive strategy can also make the optimization search effect of the algorithm more stable and accurate.

Through the testing of the ADOA algorithm, it can be concluded that the ADOA algorithm has superior capabilities in solving problems with multiple local optimal solutions and is suitable for analyzing the optimal scheduling problem of MGs.

5. Case Analysis

Table 3. Distributed Generation Devices Parameters

	Minimum capacity (kW)	Maximum capacity (kWh)	Ramping rate constrains (kW)	Capacity (kW)	Operation and maintenance (RMB/kW)
WT	5	30	-	-	0.1
PV	0	30	-	-	0.298
MT	6	30	-5/10	-	0.031
FC	3	40	-2/2	-	0.002
grid	-30	30	-	-	-
ESS	-30	30	-	200	0.012

Table 4. The Coefficients of Pollutant Emission and Treatment Price

Pollutant	Pollutant Emission (g/kWh)				Remediation cost (RMB/kg)
	MT	DE	FC	Grid	
CO_2	724	697	441	889	0.21
SO_2	0.0036	0.22	0.0022	0.8	14.84
NO_x	0.2	0.5	0.00136	0.6	62.96

Table 5. Price Flexibility

	Peak	Off Peak	Valley
Peak	-0.1	0.016	0.012
Off Peak	0.016	-0.1	0.016
Valley	0.012	0.016	-0.1

To further verify the effectiveness of the proposed method, an experimental simulation was carried out using a typical daily model of a certain MG. The basic parameters of its distributed energy sources, pollutant emission coefficients(Xie et al, 2024), and price elasticity coefficients are shown in **Table 3** and **Table 4**. The predicted output of clean energy is shown in **Figure 5**, and the electricity trading price(Dey et al,2023) and the user load curve of the MG(Dey et al, 2022) are shown in **Figure 6**. Using MATLAB to simulate the model.

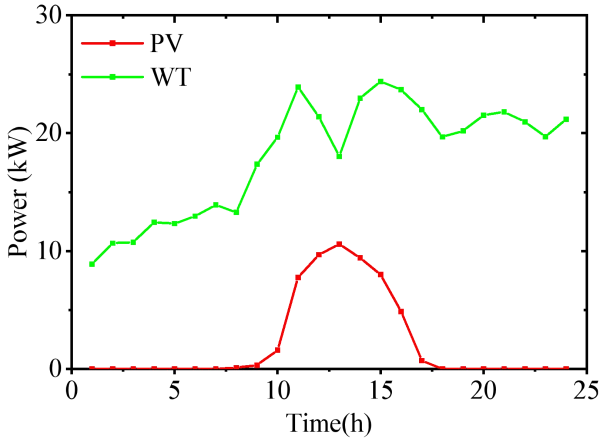

Figure 5. Predicted Output Curve of PV and WT

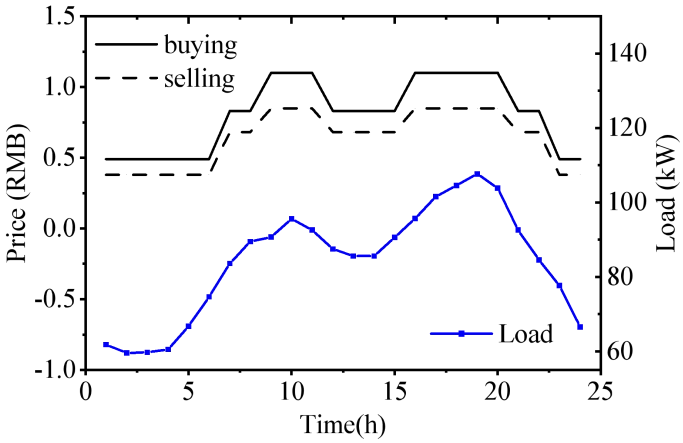

Figure 6. User Load and TOU Price

5.1 Algorithm Comparison Experiment

In order to compare the effects of the ADOA algorithm and the comparative algorithms in the MG scheduling problem, the five algorithms mentioned in the previous section were used to solve the model in this paper. The population size was set to 100, and the maximum number of iterations was set to 400. Each algorithm was independently run 20 times under the same conditions, and the average convergence curve, the optimal value, average value, standard deviation of the fitness value, the average running time, as well as the fitness value corresponding to the optimal scheduling arrangement obtained by each algorithm were recorded.

It can be seen from **Figure 7** that the convergence speeds of the five algorithms in the early stage are basically similar. The ADOA algorithm is slightly faster than the DOA algorithm, but slightly slower than the other algorithms. Even so, when the maximum number of iterations is reached, the optimal value found by the ADOA algorithm is the smallest. Therefore, it can be confirmed that when dealing

with the multi-objective scheduling problem of MGs, the ADOA algorithm can jump out of local optima to a greater extent, thus improving the quality of the solution.

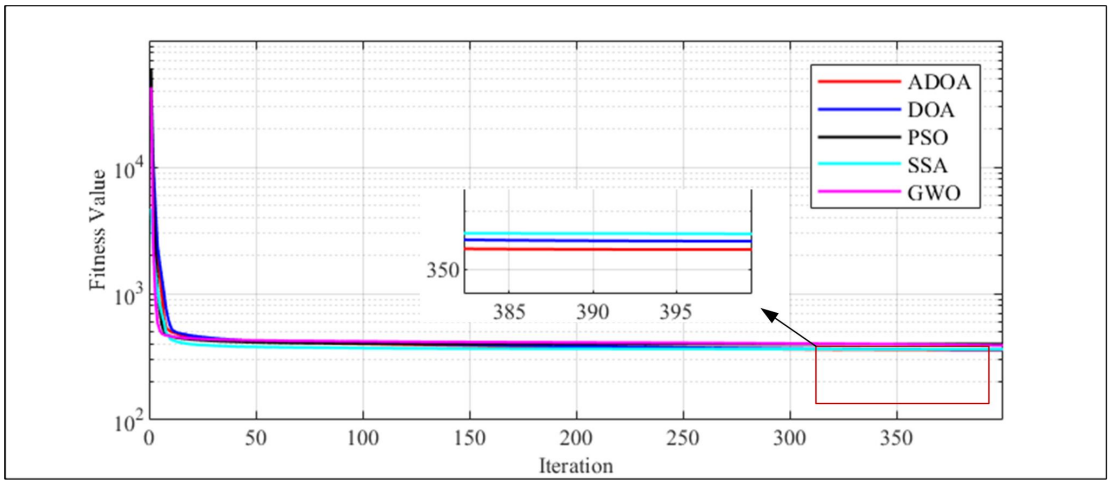

Figure 7. Algorithm Convergence Curve

Table 6. Simulation Results

Function	Algorithms	Best	Mean	Std	Tmean
F	ADOA	353.1132	356.6688	1.74603	6.0203
	DOA	355.5131	359.5700	2.1823	4.7686
	PSO	369.4908	397.9500	14.9598	5.2751
	SSA	353.9548	362.1102	5.36403	4.9013
	GWO	381.8513	388.2561	3.2520	5.6478

Table 6 records the simulation results of the five algorithms. It can be seen that ADOA comprehensively leads in terms of solution quality and solution stability, with the smallest best, mean, and standard deviation. This indicates that its improvement strategy effectively enhances the search ability. Although the computation time of ADOA is slightly longer than that of DOA and SSA, it achieves better results at a reasonable time cost, making it suitable for scenarios with high-precision requirements. As the original version of ADOA, DOA has the highest computational efficiency, but its solution quality and stability are both inferior to the improved ADOA. Its performance verifies the necessity of the improvement strategy.

Table 7 records the specific data of three types of costs corresponding to each algorithm at the optimal fitness value. In terms of power generation cost, ADOA has the lowest power generation cost, while GWO has the highest. PSO and SSA show medium-level performance. In terms of environmental cost, DOA has the best environmental protection performance, and PSO performs the worst. The difference between ADOA and DOA is extremely small (only 0.97). In terms of curtailment cost, SSA completely

avoids wind and solar curtailment, ADOA is extremely close to the optimal value, and PSO performs the worst.

Table 7. Fitness Value

Algorithms	F_1	F_2	F_3
ADOA	916.2759	145.8914	0.0962
DOA	943.8542	144.9213	0.2
PSO	923.8759	171.4377	13.1588
SSA	940.3068	150.7665	0
GWO	976.2745	164.1858	5.0938

Overall, ADOA has the lowest power generation cost, and its environmental cost and wind and solar curtailment cost are both sub-optimal. It shows the best performance in multi-objective balance and has the optimal comprehensive performance in the scenario of simultaneously optimizing the three types of costs. This verifies the superiority of ADOA in solving the multi-objective scheduling problem of MGs.

5.2 Weight Sensitivity Analysis

To study the influence of the weight configuration of the objective function on the scheduling results and verify the effectiveness of the multi-objective optimization strategy, seven additional scenarios were set up. The ADOA algorithm was independently used to solve the problems in each scenario 10 times. The weight settings of each scenario and the optimal solution results are shown in **Table 8**.

Table 8. Scenario Setting and Cost Comparison

scenarios	w	F_1	F_2	F_3	$F_1+F_2+F_3$
1	$w_1=1$, $w_2=0$, $w_3=0$	905.4721	168.7272	0.5436	1074.743
2	$w_1=0$ $w_2=1$ $w_3=0$	965.0892	123.7257	0.9077	1089.723
3	$w_1=0$ $w_2=0$, $w_3=1$	1070.4572	167.6081	0.0039	1238.069
4	$w_1=0.5$ $w_2=0.5$, $w_3=0$	944.1756	143.5812	0.2631	1090.163
5	$w_1=0$, $w_2=0.5$, $w_3=0.5$	966.7230	121.7289	0.0549	1088.507
6	$w_1=0.5$, $w_2=0$, $w_3=0.5$	931.4945	158.9391	0.2010	1090.635
7	This paper	916.2759	145.8914	0.0962	1062.264

In **Table 8**, Scenarios 1-3 are for single-objective optimization. Under single-objective optimization, the corresponding objective reaches the optimal state, but other objectives deteriorate significantly.

Scenario 1 (only F1): The power generation cost is the lowest, but the environmental cost is the highest.

Scenario 2 (only F2): The environmental cost is the lowest, but the generation cost increases by 6.58 %, and the wind and solar curtailment rises slightly.

Scenario 3 (only F3): The wind and solar curtailment is close to zero, but the generation and environmental costs soar, resulting in the highest comprehensive operation cost.

Scenarios 4-6 are for dual-objective optimization. After the weights are distributed, the comprehensive operation cost is lower than that in the single-objective scenarios, but the optimal balance is not achieved.

Scenario 4 (F1+F2): The power generation and environmental costs are balanced, but the comprehensive operation cost is still higher than that in Scenario 7.

Scenario 5 (F2+F3): The environmental cost and wind and solar curtailment perform well, but the generation cost is relatively high.

Scenario 6 (F1+F3): The power generation cost is relatively low, but the environmental cost increases significantly.

In this paper, considering the three-objective optimization, the comprehensive operation cost is the lowest, which is 12.479 lower than that in Scenario 1 (the second-best). This indicates that the algorithm is superior in global balance. It has an obvious balancing effect. The generation cost is close to the optimal value in Scenario 1 (905.47 vs 916.28), but the environmental cost and curtailment cost are moderate improved (168.7272 vs 145.8914, 0.5438 vs 0.0962). The environmental cost F2 is 13% lower than that in Scenario 1, and the curtailment cost is 89% lower than that in Scenario 2.

In summary, the weight distribution directly determines the optimization direction, but it is difficult to fully resolve multi-objective conflicts with fixed weights. The three-objective optimization mechanism of this scheduling model achieves a better global balance among generation cost, environmental cost, and wind and solar curtailment, reducing the comprehensive operation cost by 2.4%-14.2%. Specifically, compared with the situation where the cost of wind and solar power curtailment is not considered in the objective function, the cost of wind and solar power curtailment has been reduced by 63.44% to 90.38%, which verifies its effectiveness in practical applications.

5.3 Optimal Output Curve of the MG

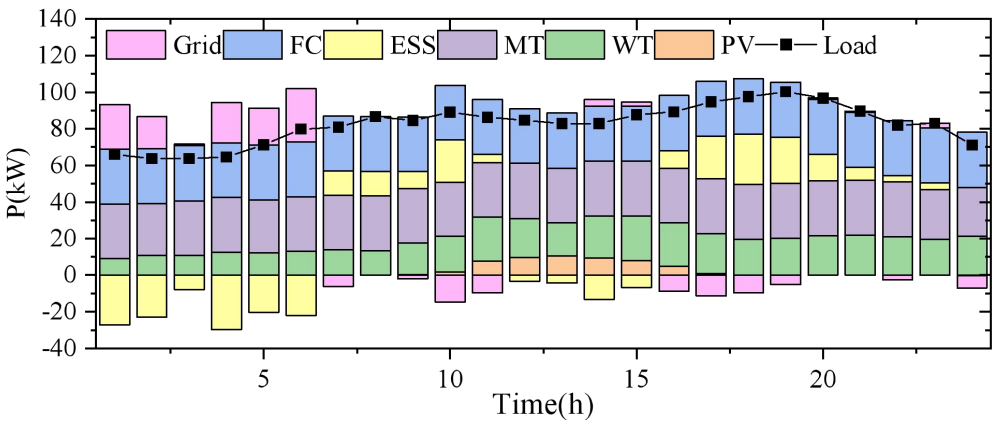

Figure 8. Equipment Output Curves

Figure 8 shows the equipment output curves corresponding to the optimal scheduling results of the MG btained by the ADOA algorithm. The output powers of PV and WT are close to their predicted outputs. During the periods from 00:00 to 06:00 and 12:00 to 15:00 when the electricity price is off-peak, priority is given to charging the ESS. When there is insufficient power in the system, electricity is purchased from the grid. From 7:00 to 11:00 and 16:00 to 22:00, the surplus power of the system is sold to the grid. Throughout the day, MT and FC operate close to full load. This is because, compared with purchasing electricity from the grid, using equipment such as MT and FC that burn natural gas is more cost-effective in terms of environmental costs during most periods.

6. Conclusion

In this paper, aiming at the problem that the MG optimization model often only considers two objectives, especially that the wind and solar curtailment cost is only used as a constraint condition and not included in the optimization objectives, a multi-objective scheduling model for MGs is proposed, which takes into account the power generation cost, environmental cost, and wind and solar curtailment cost. The improved DOA algorithm, ADOA, is used to solve the model. The comprehensive optimization performance of the proposed algorithm improvement method and the model is verified through multi-algorithm simulations and multi-scenario weight configuration experiments. The comprehensive performance of the ADOA algorithm is better than that of DOA, PSO, SSA, and GWO when solving the test functions, with obvious advantages in terms of the optimal value, average value, and standard deviation. Although it takes longer to find the optimal solution for some test functions, it can obtain higher-quality solutions. Although the introduction of the adaptive forgetting dimension slightly reduces the convergence speed, its ability to jump out of local optima and the quality of the optimization are significantly improved. In addition, the simulation results of the MG data show that the multi-objective optimization model performs excellently in the comprehensive objective optimization, reducing the comprehensive operation cost by about 2.3%-16.4%, and reducing the wind and solar power curtailment by 63.44% to 90.38%., compared with the single-objective optimization scenarios and dual-objective optimization scenarios.

Based on the above comprehensive analysis, the model and ADOA algorithm proposed in this paper can significantly enhance the environmental friendliness of the MG and the utilization rate of renewable energy, thereby making certain contributions to sustainable development.

References

Ali, A., Aslam, S., Mirsaeidi, S., Mugheri, N. H., Memon, R. H., Abbas, G., & Alnuman, H. (2024). Multi-objective multiperiod stable environmental economic power dispatch considering probabilistic wind and solar PV generation. *IET Renewable Power Generation*, *18*(16), 3903-3922. https://doi.org/10.1049/rpg2.13077

Dey, B., Raj, S., Mahapatra, S., & Márquez, F. P. G. (2022). Optimal scheduling of distributed energy

resources in microgrid systems based on electricity market pricing strategies by a novel hybrid optimization technique. *International Journal of Electrical Power & Energy Systems*, *134*, 107419. https://doi.org/10.1016/j.ijepes.2021.107419

Lang, Y., & Gao, Y. (2025). Dream Optimization Algorithm (DOA): A novel metaheuristic optimization algorithm inspired by human dreams and its applications to real-world engineering problems. *Computer Methods in Applied Mechanics and Engineering*, *436*, 117718. https://doi.org/10.1016/j.cma.2024.117718

Lin, Y., Lin, W., Wu, W., & Zhu, Z. (2023). Optimal scheduling of power systems with high proportions of renewable energy accounting for operational flexibility. *Energies*, *16*(14), 5537. https://doi.org/10.3390/en16145537

Mortazi, A., Saeed, S., & Akbari, H. (2023). Optimizing Operation Scheduling in a Microgrid Considering Probabilistic Uncertainty and Demand Response Using Social Spider Algorithm. *International Journal of Smart Electrical Engineering*, *4*(2), 113. https://doi.org/10.30495/ijsee.2022.1968838.1231

Raghavan, A., Maan, P., & Shenoy, A. K. (2020). Optimization of day-ahead energy storage system scheduling in microgrid using genetic algorithm and particle swarm optimization. *Ieee Access*, *8*, 173068-173078. https://doi.org/10.1109/ACCESS.2020.3025673

Uddin, M., Mo, H., Dong, D., Elsawah, S., Zhu, J., & Guerrero, J. M. (2023). Microgrids: A review, outstanding issues and future trends. *Energy Strategy Reviews*, *49*, 101127. https://doi.org/10.1016/j.esr.2023.101127

Wang, Y., Li, C., & Yang, K. (2020). Coordinated control and dynamic optimal dispatch of islanded microgrid system based on GWO. *Symmetry*, *12*(8), 1366. https://doi.org/10.1016/j.gloei.2024.11.008

Xie, X., Yang, H., Wang, B., Ma, Y., Zhang, D., & Shen, Y. (2024). Optimal day-ahead scheduling strategy of microgrid considering regional pollution and potential load curtailment. *Global Energy Interconnection*, *7*(6), 749-760. https://doi.org/10.1016/j.gloei.2024.11.008